Heliyon 10 (2024) e23586

Contents lists available at ScienceDirect

Heliyon

journal homepage: www.cell.com/heliyon

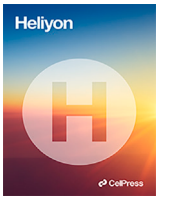

Research article

Optimal eco-driving scheme for reducing energy consumption and carbon emissions on curved roads

A.S.M. Bakibillah [a,*], M.A.S. Kamal [b,*], Chee Pin Tan [c], Tomohisa Hayakawa [a], Jun-ichi Imura [a]

[a] Department of Systems and Control Engineering, School of Engineering, Tokyo Institute of Technology, Tokyo 152-8552, Japan
[b] Graduate School of Science and Technology, Gunma University, Kiryu 376-8515, Japan
[c] School of Engineering and Advanced Engineering Platform, Monash University, Bandar Sunway 47500, Selangor, Malaysia

ARTICLE INFO

Keywords:
Eco-driving
MPC
Nonlinear optimization
Horizontal curves
Road surface conditions

ABSTRACT

Energy consumption and emissions of a vehicle are highly influenced by road contexts and driving behavior. Especially, driving on horizontal curves often necessitates a driver to brake and accelerate, which causes additional fuel consumption and emissions. This paper proposes a novel optimal ecological (eco) driving scheme (EDS) using nonlinear model predictive control (MPC) considering various road contexts, i.e., curvatures and surface conditions. Firstly, a nonlinear optimization problem is formulated considering a suitable prediction horizon and an objective function based on factors affecting fuel consumption, emissions, and driving safety. Secondly, the EDS dynamically computes the optimal velocity trajectory for the host vehicle considering its dynamics model, the state of the preceding vehicle, and information of road contexts that reduces fuel consumption and carbon emissions. Finally, we analyze the effect of different penetration rates of the EDS on overall traffic performance. The effectiveness of the proposed scheme is demonstrated using microscopic traffic simulations under dense and mixed traffic environment, and it is found that the proposed EDS substantially reduces the fuel consumption and carbon emissions of the host vehicle compared to the traditional (human-based) driving system (TDS), while ensuring driving safety. The proposed scheme can be employed as an advanced driver assistance system (ADAS) for semi-autonomous vehicles.

1. Introduction

Road transportation is a major source of energy consumption and carbon emissions worldwide. In the U.S., traffic consumes 28% of total energy [1] and emits 29% of total emissions [2]. Recent studies show that the energy consumption and carbon emissions of a vehicle are greatly influenced by road contexts [3,4] and driving behavior [5,6]. Although the driver experience is an important factor that influence the fuel consumption rate of a vehicle, it is crucial to anticipate surrounding road traffic conditions and driving states (including information on curvatures and surface conditions) to drive in an efficient-efficient manner. However, such anticipations are hardly possible for a human driver. A viable technique to address such human driving issues is *eco-driving*, which encourages energy-efficient driving behavior by preventing excessive acceleration and braking, and by optimizing the vehicle speed via anticipating

* Corresponding authors.
E-mail addresses: bakibillah.a.aa@m.titech.ac.jp (A.S.M. Bakibillah), maskamal@ieee.org (M.A.S. Kamal), tan.chee.pin@monash.edu (C.P. Tan), hayakawa@sc.e.titech.ac.jp (T. Hayakawa), imura@sc.e.titech.ac.jp (J.-i. Imura).

https://doi.org/10.1016/j.heliyon.2023.e23586
Received 23 May 2023; Received in revised form 22 November 2023; Accepted 7 December 2023

Available online 11 December 2023

surrounding road traffic conditions and driving states [7,8]. It has been demonstrated that adopting an eco-driving system can improve fuel consumption by about 4%–25% [9,10].

A number of eco-driving systems have been proposed based on road contexts. Examples of such works are those that mainly focused on rolling terrains or hilly roads [11–14]. However, the horizontal curve is another important feature of the road that significantly affects fuel consumption and carbon emissions [15]. In particular, when entering a curved road, a driver usually slows down due to safety reasons, but after passing the middle of the curve, the driver accelerates to the cruising velocity [16]. Such deceleration and acceleration increases fuel consumption and carbon emissions of the vehicle. Beckers et al. [17] developed a nonlinear model to calculate extra energy losses during motion of a vehicle in curves and showed that energy losses should not be ignored during curve maneuvering. Ko [18] reported that a vehicle moving on horizontal curves consumes 34% extra fuel and emits up to 91% more emissions when the radius is 50% lower than the minimum standard. Hence, it is crucial to develop sustainable technologies for energy-efficient driving in horizontal curves.

In the literature, several studies have developed energy-efficient driving methods for horizontally curved roads. Early work by Chang and Morlok [19] utilized the Lagrangian approach to determine the optimal vehicle speed profile on a curved road, concluding that, despite variations in road curves and other factors, the fuel consumption would be minimal for a constant speed. Similarly, Fröberg et al. [20] showed that traveling at a constant speed is the fuel-optimal approach. However, the constant speed approaches are not applicable in real-world scenarios. Polterauer et al. [21] proposed an eco-driving system considering road curvatures; however, the optimization included a constraint associated to the centripetal acceleration that indirectly restricts the maximum speed during curve maneuvering and thus, the solutions obtained are unlikely to be energy-efficient. Ikezawa et al. [22] developed an eco-driving system for electric vehicles; however, the method depends on curving stiffness of tires, which significantly varies among vehicles and tire conditions. Edrén et al. [23] developed a torque vectoring method to achieve energy-efficient curve maneuvering; however, the optimization problem is very complex and the solution may not find the global optimum. In [24], a dynamic programming (DP) approach is used to find the optimal eco-driving speed profile in circular curves, resulting in fuel savings of about 5.34% to 17.64%. Similarly, Bentaleb et al. used DP for eco-driving on curved roads [25]. While the DP-based solver yielded a global minimum, information on the entire driving cycle is required in advance and hence, the DP-based methods are incompatible for actual deployment in the real-world. Furthermore, the existing works did not consider the effect of preceding vehicles and road surface conditions in their problem formulation, and did not evaluate the energy-efficiency under dense and mixed traffic environments.

In this paper, to address the above-mentioned gaps, we develop a novel optimal eco-driving scheme using nonlinear MPC to drive a vehicle (hereafter known as the *host vehicle*) in a dense and mixed traffic environment, and evaluate its performance in a typical road with varying curvatures and surface conditions (e.g., dry, wet, and snowy). We present a method to accurately calculate road curvatures (which is crucial for effective control of the host vehicle) using global positioning system (GPS) data. To minimize fuel consumption and carbon emissions, we formulate a nonlinear optimization algorithm that dynamically calculates the optimal speed profile of the host vehicle considering its dynamics model, the state of the preceding vehicle, information of road curvatures and surface conditions, while ensuring driving safety.

The main contributions of this work are summarized as follows:

- Our proposed EDS dynamically generates the optimal speed trajectory for the host vehicle and thus, gives the energy optimal solution in horizontally curved roads.
- Our proposed method does not require prior knowledge of the entire driving cycle before the trip and hence, can be deployed in real-world.
- We evaluate the performance of the controlled host vehicle in a dense and mixed traffic environment with traditional human-driven vehicles considering various road contexts, e.g., curvatures and surface conditions.
- We analyze fuel consumption and carbon emissions of overall traffic for various penetration rates of the proposed scheme and find that the EDS significantly improves the driving performance of overall traffic (including following human-driven vehicles). Hence, this paper contributes towards the development of eco-driving techniques that can assist a group of vehicles optimize their driving strategy in the horizontally curved road.

The paper is organized as follows. In Section 2, we first describe the concept of the proposed EDS. Then, we discuss the fuel consumption and emissions model, vehicle dynamics model, the curvature calculation method, and the proposed nonlinear MPC algorithm. Section 3 presents key simulation results and discussion, followed by the conclusion and future works in Section 4.

2. Eco-driving on curved roads

The overarching concept of our proposed MPC-based optimal EDS on a horizontally curved road is illustrated in Fig. 1. The traffic environment is dense and contains both the optimally-driven (MPC-based) and human-driven (hereafter referred to as the traditional driving system (TDS)) vehicles. We make the following assumptions:

(A1) We consider a single-lane road with car-following behavior and no lane-changing or overtaking maneuver for simplicity.
(A2) We solely consider the longitudinal motion control of the host vehicle since the energy consumption and carbon emissions are directly related to the longitudinal movement.
(A3) We employ the same model for both the EDS and TDS vehicles to determine fuel consumption and carbon emissions.

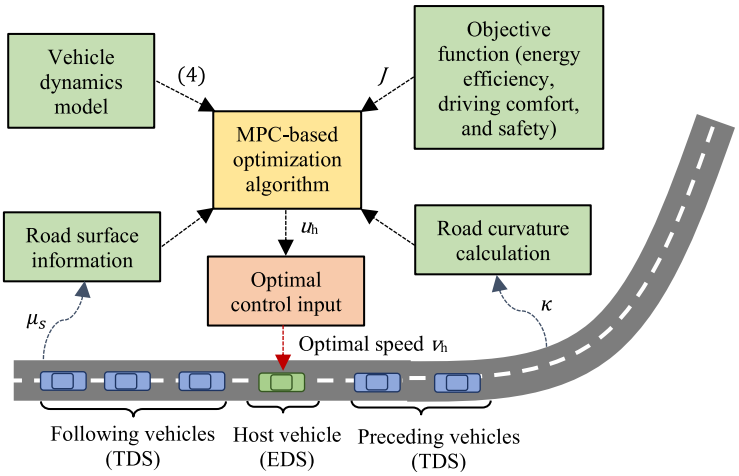

Fig. 1. The overarching concept of the proposed EDS in a horizontally curved road using nonlinear MPC. The control of the host vehicle (green) is of interest.

Table 1
The IDM parameters used in this study.

Variable	Value	Remarks
v_i^{d}	23.61 m/s	For curved segments, the desired speed is tuned
s_0	4.0 m	Kept constant
t_{id}^*	1.5 s	Realistic values range from 0.8 to 2 s
a	1 m/s^2	Realistic values range from 1 to 2 m/s^2
b	1.5 m/s^2	Realistic values range from 1 to 2 m/s^2

The EDS uses the longitudinal dynamics model of the host vehicle that incorporates the state of the preceding vehicle, information of curvatures ahead, and surface conditions to calculate the optimal speed that minimizes fuel consumption and carbon emissions. The GPS is used to determine the location of the host vehicle, while car-mounted sensors provide information on road surface conditions. The coordinates (longitude and latitude) of the entire route are considered to be available, which are then used to calculate the road curvature. Note that the digital map can be used to obtain the GPS coordinates of a route.

The human-driven vehicles are modeled using a microscopic car-following model called the Intelligent Driver Model (IDM) [26]. The IDM is often used to study various traffic situations since it properly models the human driving behavior. Using IDM as in (1), the immediate acceleration $u_i(t)$ of the TDS vehicle i with respect to its preceding vehicle $i-1$ is computed as

$$\begin{aligned} u_i(t) &= f(v_i(t), x_i(t), v_{i-1}(t), x_{i-1}(t), v_i^{\mathrm{d}}) \\ &= a\left[1 - \left(\frac{v_i(t)}{v_i^{\mathrm{d}}(t)}\right)^4 - \left(\frac{s^*(v_i(t), \Delta v_i(t))}{\Delta x_i(t)}\right)^2\right], \\ s^*(v_i, \Delta v_i) &= s_0 + v_i t_{\mathrm{id}}^* + \frac{v_i \Delta v_i}{2\sqrt{ab}}, \end{aligned} \tag{1}$$

where x_i, v_i, v_i^{d}, s_0, t_{id}^*, a, and b are the position, velocity, desired speed, minimum gap, safe time headway, maximum acceleration, and comfortable braking, respectively, of TDS vehicle i and $\Delta x_i = x_i - x_{i-1}$ and $\Delta v_i = v_i - v_{i-1}$ are the actual distance and speed difference between adjacent vehicles, respectively. The parameters of the IDM used in this study are given in Table 1.

Note that the IDM can describe the acceleration in terms of the position and speed dynamics of the vehicle, but cannot directly change the speed with respect to the curvature. Hence, we regulate the desired speed v_i^{d} of the IDM based on the curve speed limit (as given in (2)) to incorporate the effect of curvature in the input acceleration of the TDS vehicles as

$$v_i^{\mathrm{d}}(t) = \begin{cases} \beta v_{\mathrm{c,lim}}(x_i(t-1)) + (1-\beta)v_i^{\mathrm{d}}(t-1), & \text{if } v_i^{\mathrm{d}}(t-1) > v_{\mathrm{c,lim}}(x_i(t-1)), \\ \min(v_{\mathrm{c,lim}}(x_i(t-1)), v_{\mathrm{R,max}}), & \text{otherwise}, \end{cases} \tag{2}$$

where $\beta < 1$ is the multiplication factor used to progressively slow down the vehicle on the curve, $v_{\mathrm{c,lim}}(x_i)$ is the speed limit of the curved segment, and $v_{\mathrm{R,max}}$ is the speed limit of the straight road. The goal of this paper is to develop an optimal eco-driving driving scheme for reducing fuel consumption and carbon emissions on horizontally curved roads for different surface conditions in a dense and mixed traffic environment. The following sections describe fuel consumption and emissions model, vehicle dynamics model, curvature calculation method, the objective function, and the control method in detail.

2.1. Fuel consumption and emissions model

Over the past decades, several fuel consumption and emissions models have been developed [27,28]. The variations in fuel consumption and emissions from different models are mainly due to the type and properties of the vehicle being modeled. In this paper, we employ the VT-Micro model [29,30] to calculate the fuel consumption and emissions of a vehicle based on its instantaneous speed and acceleration. The model was developed at Oak Ridge National Laboratory (ORNL) from experiments with nine regular emitting light-duty vehicles and various polynomial combinations of velocity and acceleration were investigated under this model using chassis dynamo-meter data acquired at the ORNL. Specifically, the data included between 1300 and 1600 unique measurements for each vehicle and Measure of Effectiveness (MOE) combination depending on the vehicle's operating envelope. The VT-Micro model is well-known for its simple structure and is widely used in transportation studies to evaluate fuel consumption and emissions [31,32]. Hence, we choose the VT-Micro model to investigate fuel consumption and carbon emissions of vehicles and is given as

$$\ln(MOE_{ei}) = \sum_{l=0}^{3}\sum_{m=0}^{3}(K_{l,m}^{e} v_i^l u_i^m), \tag{3}$$

where MOE_{ei} is the fuel consumption and emissions rates of vehicle i, $K_{l,m}^{e}$ is the regression coefficient, l and m are the power of speed and acceleration, respectively. The regression coefficients $K_{l,m}^{e}$ are calibrated using the ORNL field data [30] and are given in [31]. The trajectory data of the vehicle, which contains the speed and acceleration at each simulation time-step, can be used as the input of (3) to calculate the fuel consumption and emissions of vehicles.

2.2. Vehicle dynamics model

In this section, we present the vehicle dynamics and operational hypotheses to design an MPC controller. Since energy consumption is directly related to the longitudinal movement, we solely consider the longitudinal motion control for eco-driving. The nonlinear state equation of the vehicle control system (including the state of the preceding vehicle) at time t is given by

$$\dot{z}(t) = f(z(t), u_{\mathrm{h}}(t), q(t)), \tag{4}$$

where $z(t) = [x_{\mathrm{h}}(t), v_{\mathrm{h}}(t), x_{\mathrm{p}}(t), v_{\mathrm{p}}(t)]^{\mathrm{T}} \in \mathbb{R}^4$ is the state vector with x_{h} and v_{h} being the position and velocity (respectively) of the host vehicle, and x_{p} and v_{p} being the position and velocity of the preceding vehicle, $u_{\mathrm{h}} \in \mathbb{R}$ is the control input associated with the traction force, which is applied to the host vehicle, and $q(t) = \dot{v}_{\mathrm{p}}(t)$ is a time varying parameter that represents acceleration of the preceding vehicle $a_{\mathrm{p}}(t)$ that is computed by the measured velocity $v_{\mathrm{p}}(t)$.

When the host vehicle is operating in traction mode, its longitudinal motion is subject to the total forces acting on it, and is represented by

$$m_{\mathrm{h}} \frac{\mathrm{d}v_{\mathrm{h}}(t)}{\mathrm{d}t} = F_{\mathrm{h}}^{\mathrm{T}}(t) - F_{\mathrm{h}}^{\mathrm{R}}(t), \tag{5}$$

where m_{h} is the equivalent mass, $F_{\mathrm{h}}^{\mathrm{T}}(t)$ is the traction force, and $F_{\mathrm{h}}^{\mathrm{R}}(t)$ is the sum of all motion resistance forces. The traction force in (5) is equivalent to the product of the mass and the resulting acceleration as $F_{\mathrm{h}}^{\mathrm{T}}(t) = m_{\mathrm{h}} u_{\mathrm{h}}(t)$. The motion resistance forces include aerodynamic drag, rolling resistance, and gravitational force, and are given by $F_{\mathrm{h}}^{\mathrm{R}}(t) = \frac{1}{2} C_{\mathrm{d}} \rho_{\mathrm{a}} A_{\mathrm{h}} v_{\mathrm{h}}^2(t) + \lambda m_{\mathrm{h}} g \cos\theta(t) + m_{\mathrm{h}} g \sin\theta(t)$, where C_{d} is the drag coefficient, ρ_{a} is the air density, A_{h} is the frontal area of the vehicle, λ is the rolling resistance coefficient, g is the gravitational acceleration, and θ is the road inclination angle. We assume that the road inclination angle θ is very small at any point on the road and thus, $\cos\theta \approx 1$ and $\sin\theta \approx \theta$.

Hence, the nonlinear state equation (4) of the host vehicle can be written as

$$f(z(t), u_{\mathrm{h}}(t), q(t)) = \begin{bmatrix} v_{\mathrm{h}}(t) \\ -\frac{1}{2m_{\mathrm{h}}} C_{\mathrm{d}} \rho_{\mathrm{a}} A_{\mathrm{h}} v_{\mathrm{h}}^2(t) - \lambda g - g\theta(t) + u_{\mathrm{h}}(t) \\ v_{\mathrm{p}}(t) \\ q(t) \end{bmatrix}, \tag{6}$$

where the term $-\frac{1}{2m_{\mathrm{h}}} C_{\mathrm{d}} \rho_{\mathrm{a}} A_{\mathrm{h}} v_{\mathrm{h}}^2(t) - \lambda g - g\theta(t) + u_{\mathrm{h}}(t)$ is the apparent acceleration of the host vehicle. The control input $u_{\mathrm{h}}(t)$ is applied through its throttle or brake (for acceleration and braking). The purpose of controlling the motion of the host vehicle is to enhance fuel efficiency and reduce carbon emissions (while ensuring driving safety) based on the status of the preceding vehicle, information on upcoming curves, and surface conditions. Our longitudinal motion dynamical model (6) enables fast optimization, allowing for real-time implementation. Note that we do not consider the lateral dynamics in the model, as the lateral motion has negligible effect on fuel consumption and emissions, in addition to the fact that incorporating lateral dynamics into longitudinal motion control will make the formulation and optimization unnecessarily complex.

Table 2
Category of horizontal curve radius.

Radius type	Radius length [m]	Operating speed [km/h]
Small	< 150	< 70
Medium	150 – 850	70 – 120
Large	> 850	> 120

2.3. Road curvature calculation

On a roadway, curvatures of different radii are usually encountered. The radius of horizontal curves can be categorized as small, medium, and large radius as given in Table 2. There are different methods (e.g., field survey, chord length, ball bank indicator, plan sheet, GPS, operating speed, and vehicle yaw rate) to estimate road curvatures. The most common method is to use a series of plan sheets kept by the local transportation department. Although this is clearly a viable method for determining curve radius, it is time intensive and thus, cannot be used for real-time control. Also, accessibility to such data is often quite challenging. In functional terms, the plan sheet method and the GPS approach provide the lowest mean relative errors for estimating the curve radius as −0.9% and 1.2%, respectively [33].

Here we present a method to reliably calculate the road curvature based on high-precision GPS coordinate (X, Y) data readily available from a digital map. In particular, we calculate the curvature by fitting circular curves with three successive coordinate points by assuming that the curvature between these points is uniform; this assumption is not restrictive if the measurement interval is small. Assuming that a road has coordinates (X_1, Y_1), (X_2, Y_2), and (X_3, Y_3); which can be used to form a circular curve with a radius of R_c by solving three equations for three unknowns as in (7) and is given as

$$\begin{bmatrix} X_1 & Y_1 & 1 \\ X_2 & Y_2 & 1 \\ X_3 & Y_3 & 1 \end{bmatrix} \begin{bmatrix} a \\ b \\ c \end{bmatrix} = \begin{bmatrix} -(X_1^2 + Y_1^2) \\ -(X_2^2 + Y_2^2) \\ -(X_3^2 + Y_3^2) \end{bmatrix}. \tag{7}$$

Then, the radius R_c and curvature κ are calculated as $R_c = \sqrt{a^2 + b^2 - 4c}$ and $\kappa = 1/R_c$. A large κ indicates sharp turning and vice versa. The critical velocity $v_{c,\kappa}$ (the maximum velocity at which a curve can be negotiated) as a function of radius can be given as $v_{c,\kappa} = f\left(R_c(x_h)\right) \approx \zeta f(x_h)$, where $\zeta < 1$ is a positive threshold. For various surface conditions (e.g., dry, wet, and snow) $v_{c,\kappa}$ can be calculated as [34] $v_{c,\kappa}(x_h) = \sqrt{\mu_s g R_c(x_h)}$, where μ_s is the road surface friction coefficient (lateral friction coefficient). Note that $v_{c,\kappa}$ significantly varies with the variation of R_c along the curve. Furthermore, $v_{c,\kappa}$ is highly influenced by μ_s due to considerable change in the friction supply to tires. To effectively control a vehicle on the horizontally curved road, it is necessary to consider $v_{c,\kappa}$ in the optimization problem as described in the next section.

2.4. Model predictive control

The acceleration and deceleration (braking) of a vehicle are directly coupled to the input force and engine torque fluctuation, and excessive acceleration/braking is undesirable because it increases fuel usage and carbon emissions whilst reducing passenger comfort. The proposed MPC-based EDS generates the optimal velocity trajectory for efficient and safe driving within a prediction horizon using instantaneous states of the vehicles and road contexts. The optimization algorithm includes practical constraints of velocity, acceleration, and safe headway. Due to dynamic nature of traffic flow, a suitable prediction horizon (analogous to human driver's anticipation) needs to be considered; for instance, a long horizon is not appropriate if traffic flow changes rapidly. The safe headway of the host vehicle s_d from the preceding vehicle is defined as $s_d(t) = s_0 + t_{hd}^* v_h(t)$, where s_0 is the minimum gap between vehicles and t_{hd}^* is the safe (reference) time headway when following the preceding vehicle.

The nonlinear MPC is implemented by minimizing the following objective function at each time t with state dynamics (4) and (6) as

$$\begin{aligned} J(z(t), u_h(\cdot)) = \int_t^{t+T} & [w_1 (v_h(\tau) - v_d)^2 + w_2 u_h^2(\tau) \\ & + w_3 \left(1 + e^{-\sigma(t_{hd}^* - t_{hd}(\tau))}\right)^{-1}] \, d\tau, \end{aligned} \tag{8}$$

subject to

$$\begin{aligned} & t \le \tau \le t + T, \\ & v_{min} \le v_h(\tau) \le v_{max,c}(x_h(\tau)), \\ & u_{min} \le u_h(\tau) \le u_{max}, \\ & x_p(\tau) - x_h(\tau) \ge s_d(\tau), \end{aligned}$$

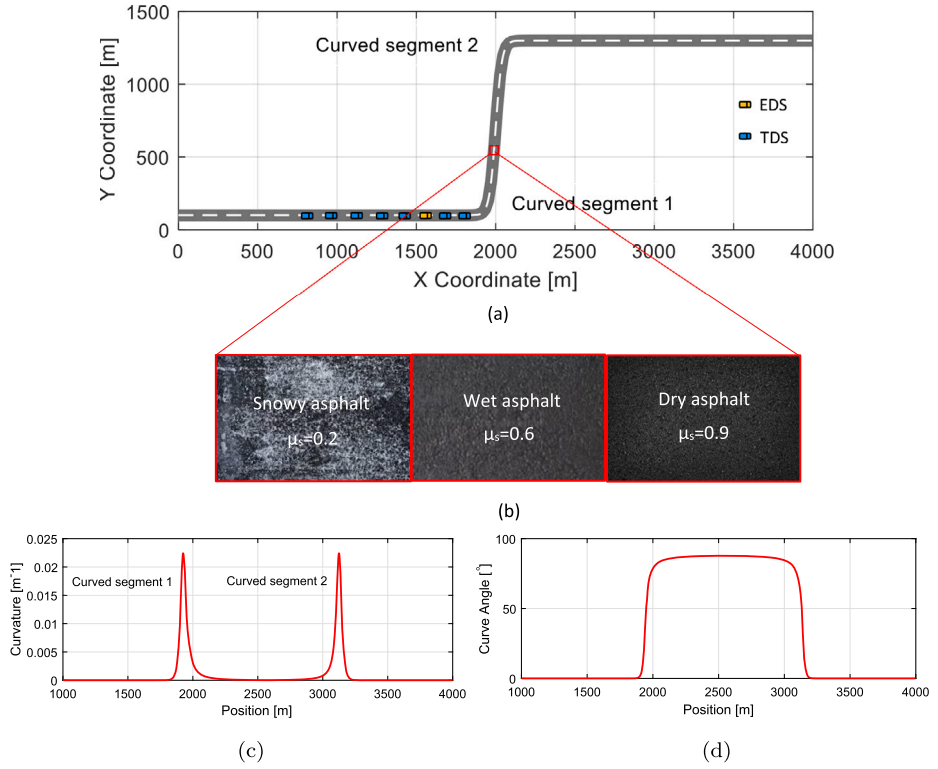

Fig. 2. (a) The study horizontally curved road profile, (b) surface conditions of the track, (c) curvatures, and (d) curve angle. The friction coefficient μ_s varies significantly depending on surface conditions.

where T is the prediction horizon over which the optimal trajectories are determined, v_d is the constant desired velocity throughout the freeway, $\sigma \in \mathbb{R}_+$ is a constant, $t_{hd}(\tau) = (x_p(\tau) - x_h(\tau) - s_0)/(v_h(\tau) + \gamma)$ is the instantaneous headway where $\gamma \in \mathbb{R}_+$ avoids singularity at $v_h(t) = 0$, and w_1, w_2, and w_3 are the weights of the velocity, acceleration, and safe headway terms, respectively. The maximum velocity at different locations of the freeway is determined as $v_{max,c}(x_h) = \min(v_{c,\kappa}(x_h), v_{R,max})$. The first term of (8) is the penalty when the speed of the host vehicle deviates from v_d and the second term is the cost of acceleration along the curve, whereas the third term represents a penalty due to deviation from the reference headway (to ensure driving safety), which increases if the host vehicle moves closer to the preceding vehicle, and vice versa. Smooth speed variations relating to the preceding vehicle, road curvature, and surface conditions have the potential to greatly improve the fuel economy and emissions of the host vehicle.

2.5. Simulation model and settings

To demonstrate the efficacy of the proposed EDS, we developed a simulation model in MATLAB (which has been used to simulate numerous real-world events). Then, we solved the nonlinearly constrained optimization problem (8) in discrete time using the nonlinear programming solver called *find minimum of constrained nonlinear multivariable function (fmincon)* in the MATLAB optimization toolbox. For a faster and more accurate solution, we have used the sequential quadratic programming (SQP) algorithm in the *fmincon* solver. The vehicle parameters are chosen as $m_h = 1200$ kg, $C_d = 0.32$, $\rho_a = 1.184$ kg/m^3, $A_h = 2.5$ m^2, $g = 9.8$ m/s^2, and $\lambda = 0.015$. We set the safe headway time t^*_{hd} and minimum spacing s_0 for the MPC to be respectively 1.5 s and 4 m. The desired velocity v_d of the MPC is set at 23.61 m/s (85 km/h), and the velocity and acceleration constraints are respectively set as $v_h \in [0, 25]$ m/s and $u_h \in [-5, 2]$ m/s^2. The simulations are run for 500 s with a traffic volume of 800 veh/h. The simulation step is set at $dt = 0.5$ s, with a prediction horizon of $T = 20$ s, divided into 40 steps. The initial velocity v_h of the host vehicle is set at $v_h(0) = 22.23$ m/s. The weights w_1, w_2, and w_3 in the objective function (8) are set as 0.15, 15, and 40, respectively. Note that the weight values w_1 and w_2 are determined in such a way that retain the domination of velocity and acceleration in similar scale (since they are squared terms), whereas the weight value w_3 is chosen a high value that dominates other terms only in safety critical situations (to ensure driving safety). Then, the weight values w_1 and w_2 are further tuned based on the performance improvement in fuel economy and carbon emissions.

The performance of the proposed optimal EDS is evaluated using microscopic traffic simulations considering road context information (curvatures and surface conditions) of a typical horizontally curved road as shown in Fig. 2(a) in a dense and mixed traffic with TDS vehicles. We consider that the study curved road is single-lane and the surface condition can be dry, wet, or snowy. The texture and friction coefficients for various surface conditions are shown in Fig. 2(b). We consider real values of friction coefficients μ_s for different surface conditions measured by vehicle mounted sensors [35]. The curvature and the curve angle are depicted in

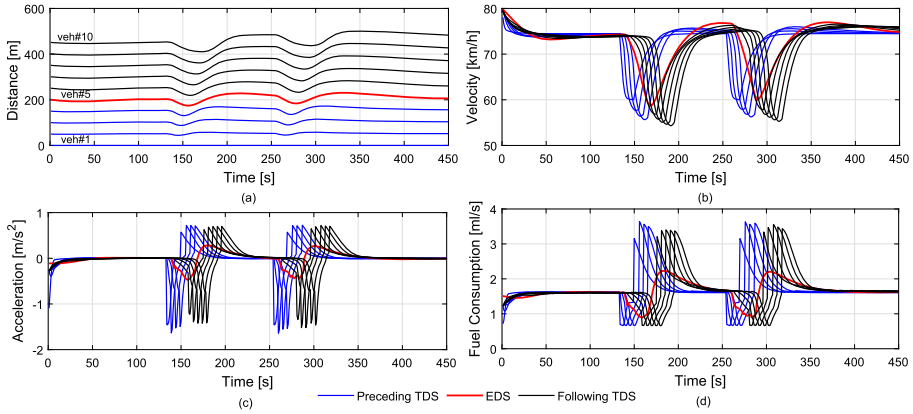

Fig. 3. Drive along the study road under dry surface condition. The sub-figures show (a) inter-vehicle gaps, (b) velocity profiles, (c) acceleration profiles, and (d) instantaneous fuel consumption of the TDS and EDS vehicles.

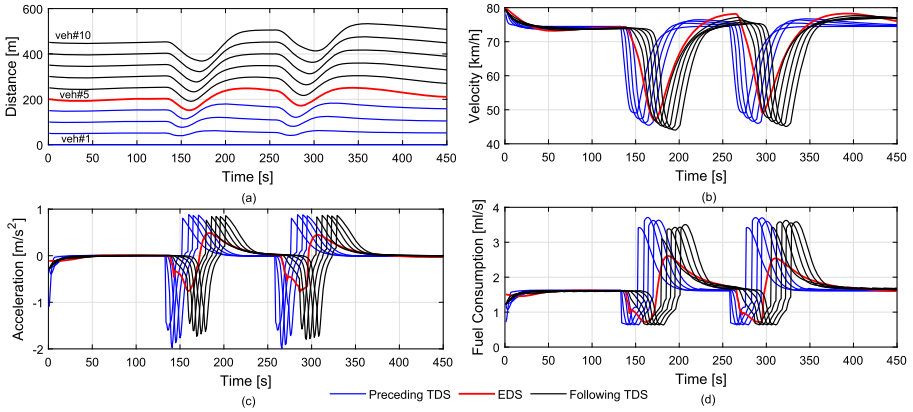

Fig. 4. Drive along the study road under wet surface condition. The sub-figures show (a) inter-vehicle gaps, (b) velocity profiles, (c) acceleration profiles, and (d) instantaneous fuel consumption of the TDS and EDS vehicles.

Fig. 2(c) and (d), respectively. Since the smallest curve radius of the study road is observed to be 45 m (Fig. 2(c)), the curves are categorized as small radius according to Table 2. Note that, due to the dynamic nature of traffic flows in real-world scenarios, we conduct simulation experiments multiple times with different seeds of random number generation of the simulator and average the results to avoid randomness influencing the simulation results. In particular, we simulate the same group of experiments (for each road surface condition) ten times with various random seeds.

For demonstration, we consider a group of ten vehicles in a synchronous, dense, and mixed traffic condition, where the fifth vehicle is an EDS vehicle (MPC-based), and the preceding and following vehicles are the TDS vehicles (human-driven). We suppose that the first TDS vehicle is traveling at a lower speed (75 km/h) (due to dense traffic) than the desired speed of the EDS vehicle and adjusting its speed (slow down) at the exact location on the curve. Hence, the following TDS and EDS vehicles also need to adjust their speeds accordingly. The braking effect of the first TDS vehicle causes other following vehicles to brake quickly and this effect propagates backward creates *shock wave*. The goal is to determine (i) how energy-efficient the EDS vehicle is concerning road contexts (i.e., curvatures and surface conditions) while following the traditional vehicles (preceding TDS), (ii) how capable the EDS vehicle is to alleviate the braking effect/shock wave on curved roads in a dense traffic scenario, and (iii) what is the impact of the EDS vehicle on its following TDS vehicles and overall traffic for its different penetration rates?

3. Simulation results and discussion

3.1. Performance evaluation in dense and mixed traffic

The simulation results for the TDS and EDS vehicles traveling on the study horizontally curved road under dry ($\mu_s = 0.9$), wet ($\mu_s = 0.6$), and snowy ($\mu_s = 0.2$) surface conditions are illustrated in Figs. 3(a)–(d), 4(a)–(d), and 5(a)–(d), respectively. It is observed that when approaching the curve, the TDS vehicles slow down quickly by generating appropriate control actions and then immediately accelerate back to the initial velocity. Such rapid variations in motion, deceleration, and acceleration affect fuel consumption and emissions of the TDS vehicles. On the other hand, the EDS vehicle slows down steadily by anticipating the behavior

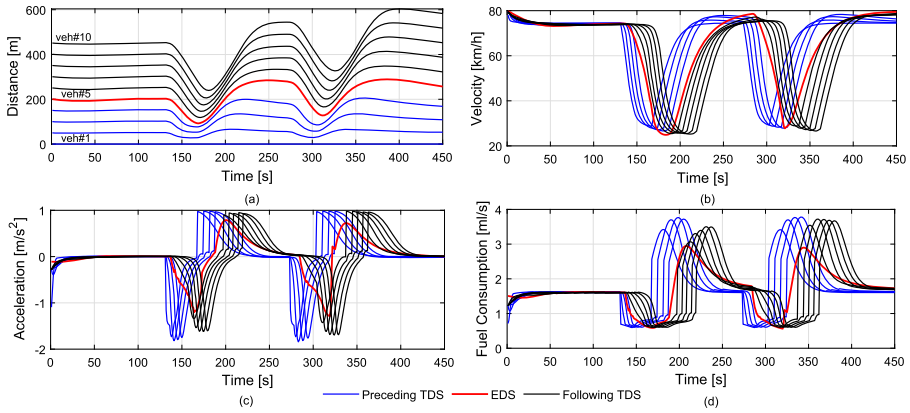

Fig. 5. Drive along the study road under snow surface condition. The sub-figures show (a) inter-vehicle gaps, (b) velocity profiles, (c) acceleration profiles, and (d) instantaneous fuel consumption of the TDS and EDS vehicles.

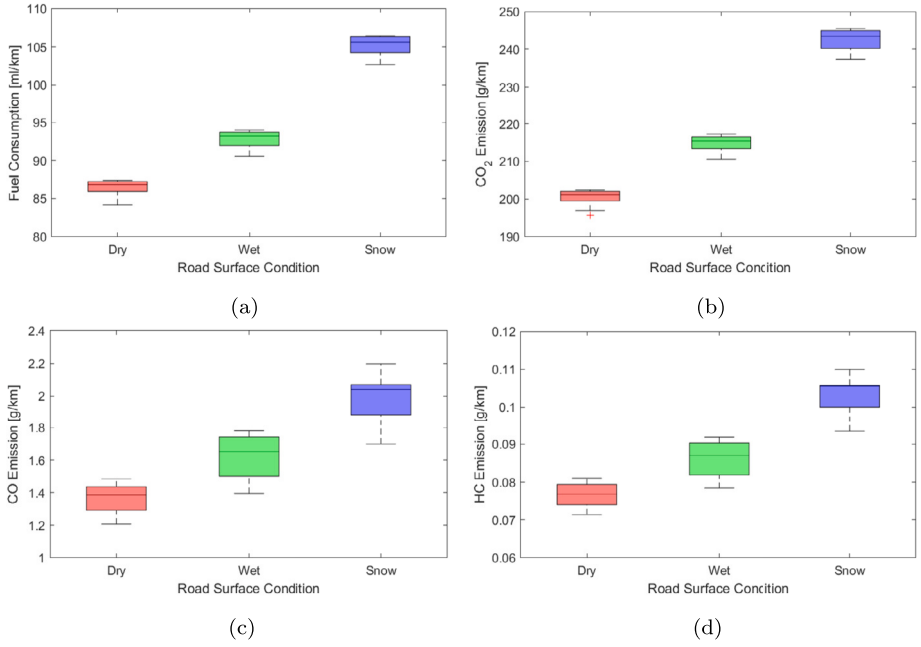

Fig. 6. Distributions of (a) fuel consumption, (b) CO_2 emission, (c) CO emission, and (d) HC emission rates of the TDS and EDS vehicles for different road surface conditions.

of its preceding vehicles as it approaches the curve and then gradually accelerates to reach its cruising velocity. Note that the road surface conditions affect human driving behavior along with the curvature effect. Specifically, when the surface friction μ_s (to tires) is low (e.g., wet and snowy surface conditions), the critical velocity $v_{c,\kappa}$ decreases significantly and a driver may need to deliver an extra effort to control the vehicle on curves. Such actions increase the acceleration and/or deceleration rates of the vehicle (as shown in Fig. 4(c) and 5(c)), which may also cause additional fuel consumption and carbon emissions as illustrated in Fig. 6(a)–(d).

Fig. 7(a)–(d) respectively shows the fuel consumption, and CO_2, CO, and HC emission rates of each TDS and EDS vehicles for driving on the study road under dry, wet, and snowy surface conditions. We find that the surface conditions have a substantial impact on vehicle fuel consumption and carbon emissions along with the curvature, and for all conditions, the EDS performs significantly better than the TDS. Specifically, for dry, wet, and snowy surface conditions, the proposed MPC-based EDS outperforms the immediate preceding TDS by 3.4%, 3.6%, and 3.9%, respectively, in reducing fuel consumption, 3.2%, 3.4%, and 3.5%, respectively, in CO_2 emission reduction, 18.9%, 22.4%, and 24.5%, respectively, in CO emission reduction, and 12.3%, 16.2%, and 18.6%, respectively, in HC emission reduction. This is because the EDS vehicle smoothly adjusts its velocity while traversing the curved segment and keeps the acceleration (control input) at the optimal level for different surface conditions, while precisely anticipating the behavior of preceding vehicles. These findings demonstrate the novelty of the proposed EDS compared to the TDS in reducing fuel consumption, and carbon emissions on curved roads.

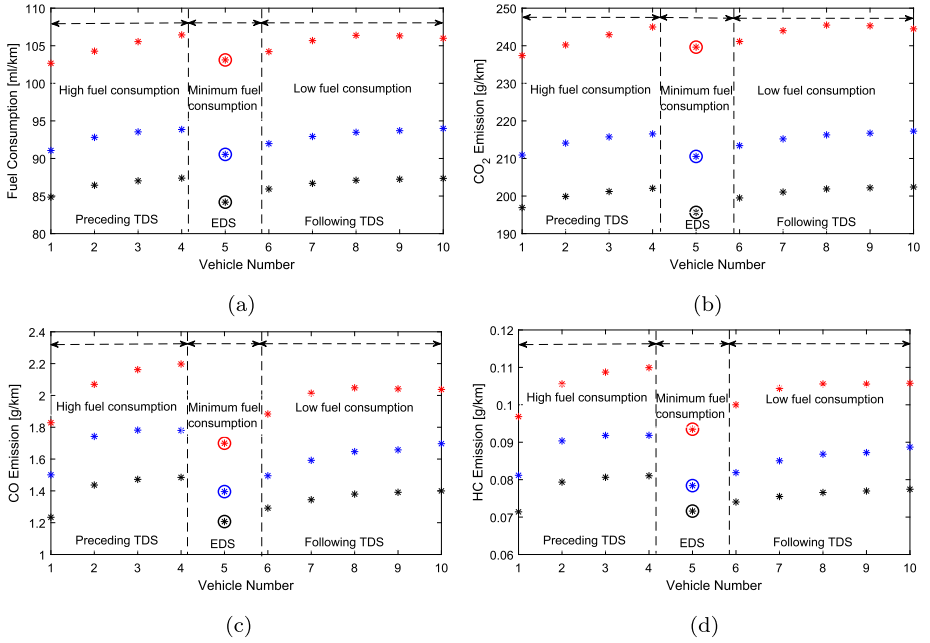

Fig. 7. Performance evaluation (a) fuel consumption, (b) CO_2 emission, (c) CO emission, and (d) HC emission rates of each TDS and EDS vehicles while traveling on the study road. The black, blue, and red stars respectively denote the dry, wet, and snowy surface conditions.

Moreover, we find that the proposed EDS significantly improves the driving performance of its following TDS vehicles. Specifically, the fuel consumption of the first following vehicle (6th TDS) is reduced by 1.6%, 2.2%, and 2.8% compared to the immediate preceding vehicle (4th TDS) of the EDS for dry, wet, and snow surface conditions, respectively. Consequently, the CO_2 emission is reduced by 1.2%, 1.5%, and 1.8%, the CO emission is reduced by 12.8%, 16.9%, and 18.1%, and the HC emission is reduced by 8.6%, 10.8%, and 12.6%. This improvement is due to the fact that the EDS vehicle administers the following TDS vehicles to follow the suit and travel in the optimal ecological way. As a result, the proposed EDS significantly reduces fuel consumption and carbon emissions of following TDS vehicles. These findings motivate the evaluation of overall traffic performance for various penetration rates of EDS vehicles.

3.2. Impact of various EDS penetration rates

We evaluate the effect of various penetration rates of the EDS vehicles on the overall fuel consumption and carbon emissions under dense and mixed traffic environment with TDS vehicles. The penetration rates of the EDS vehicles are varied from 0% to 100%, with a step of 20%. Then, the trajectory data are generated using numerical simulations for various surface conditions. Specifically, we calculate the average fuel consumption rate, and average CO_2, CO, and HC emission rates for varying EDS penetration rates for dry, wet, and snowy surface conditions as given in Table 3.

It is found that as the EDS penetration rate is increased, the fuel consumption and carbon emissions reduce progressively for all surface conditions, which suggests that using the EDS to manage mixed traffic flow on horizontally curves can significantly reduce fuel consumption and carbon emissions. Fig. 8(a)–(d) respectively illustrates the percentage reductions of average fuel consumption, and average CO_2, CO, and HC emissions for different penetration rates of EDS vehicles on the study horizontally curved road.

4. Conclusion

In this paper, a novel optimal MPC-based EDS has been developed for a host vehicle traveling on a typical horizontally curved road in a dense and mixed traffic environment with traditional human-driven vehicles. A nonlinear optimization problem is formulated considering the longitudinal motion dynamics of the host vehicle, the state of the preceding vehicle, and information of road curvature and surface conditions to improve vehicle fuel efficiency and carbon emissions, while ensuring safe driving. The EDS vehicle smoothly varies its velocity by maintaining adequate deceleration when traversing the curved segment and then accelerates with an appropriate acceleration level to reach its cruising velocity, ensuring the least amount of energy wasted during acceleration and braking. Hence, the EDS has caused a significant reduction in fuel consumption and carbon emissions compared to the TDS. Moreover, the EDS substantially reduces the fuel consumption and carbon emissions of following TDS by assuring an appropriate driving strategy. The fuel consumption and carbon emissions of vehicles decrease progressively with the increase of the EDS penetration rates, which indicates that the application of EDS can improve the overall traffic performance on horizontally curved roads for different surface conditions.

Table 3
Average fuel consumption and carbon emission rates for varying EDS penetration rates and surface conditions.

Fuel consumption and carbon emissions	EDS penetration rates					
	0%	20%	40%	60%	80%	100%
Dry surface:						
FC (ml/km)	87.20	85.84	84.92	84.22	83.48	83.22
CO_2 (g/km)	201.86	199.12	197.20	194.98	194.01	192.68
CO (g/km)	1.44	1.32	1.26	1.22	1.18	1.15
HC (g/km)	0.079	0.075	0.072	0.069	0.066	0.064
Wet surface:						
FC (ml/km)	93.98	92.23	91.12	90.22	89.46	89.10
CO_2 (g/km)	217.54	214.16	211.44	209.62	207.73	205.94
CO (g/km)	1.73	1.58	1.46	1.41	1.34	1.32
HC (g/km)	0.094	0.088	0.084	0.081	0.079	0.078
Snowy surface:						
FC (ml/km)	106.54	104.02	102.45	101.74	101.18	100.16
CO_2 (g/km)	244.85	240.42	236.58	234.15	232.28	230.95
CO (g/km)	2.14	1.92	1.78	1.70	1.64	1.61
HC (g/km)	0.109	0.101	0.096	0.091	0.089	0.088

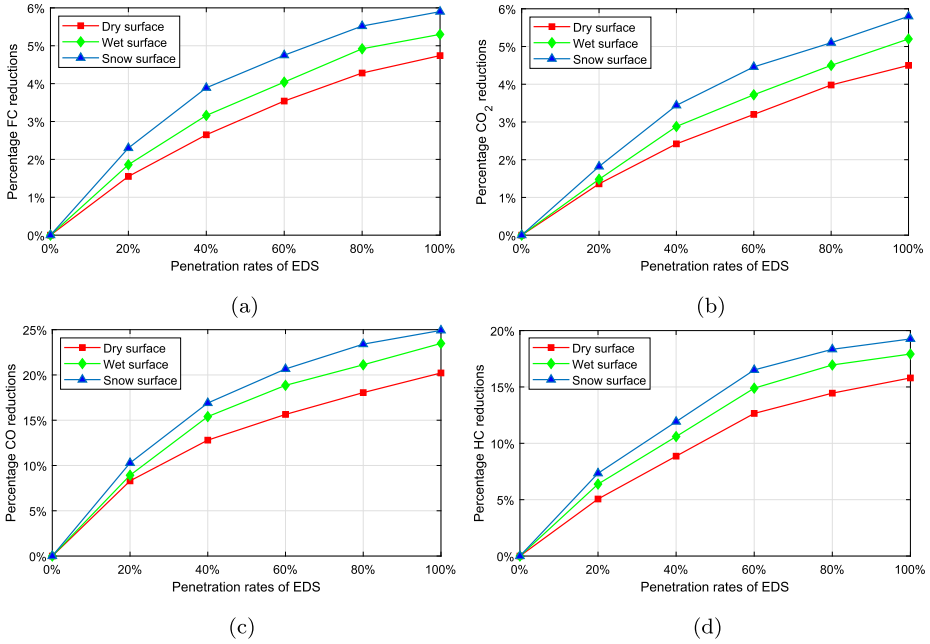

Fig. 8. Percentage reductions of average (a) fuel consumption, (b) CO_2 emission, (c) CO emission, and (d) HC emission for different penetration rates of EDS vehicles.

Our future work aims to extend the model for multi-lane traffic scenarios and incorporate inter-vehicle communications. Also, applying our method to electric vehicles would be an interesting future study.

CRediT authorship contribution statement

A.S.M. Bakibillah: Conceptualization, Formal analysis, Methodology, Writing – original draft. **M.A.S. Kamal:** Conceptualization, Formal analysis, Funding acquisition, Methodology, Writing – review & editing. **Chee Pin Tan:** Project administration, Writing – review & editing. **Tomohisa Hayakawa:** Writing – review & editing. **Jun-ichi Imura:** Funding acquisition, Writing – review & editing.

Declaration of competing interest

The authors declare that they have no known competing financial interests or personal relationships that could have appeared to influence the work reported in this paper.

Data availability

No data was used for the research described in the article.

Acknowledgement

This research is supported by the Japan Society of the Promotion of Science (JSPS) Grant-in-Aid for Scientific Research (C) 23K03898.

References

[1] U.S. EIA, Annual Energy Outlook 2019: with Projections to 2050, U.S. Department of Energy, 2019.
[2] U.S. EPA, Inventory of U.S. Greenhouse Gas Emissions and Sinks: 1990-2017, Environmental Protection Agency, 2019.
[3] M.V. Faria, G.O. Duarte, R.A. Varella, T.L. Farias, P.C. Baptista, How do road grade, road type and driving aggressiveness impact vehicle fuel consumption? Assessing potential fuel savings in Lisbon, Portugal, Transportation Research Part D: Transport and Environment 72 (2019) 148–161.
[4] A. Beji, K. Deboudt, S. Khardi, B. Muresan, L. Lumière, Determinants of rear-of-wheel and tire-road wear particle emissions by light-duty vehicles using on-road and test track experiments, Atmospheric Pollution Research 12 (3) (2021) 278–291.
[5] Y. Huang, E.C. Ng, J.L. Zhou, N.C. Surawski, X. Lu, B. Du, E.F. Chan, Impact of drivers on real-driving fuel consumption and emissions performance, Science of the total environment 798 (2021) 149297.
[6] N.B. Dhital, S.X. Wang, C.H. Lee, J. Su, M.Y. Tsai, Y.J. Jhou, H.H. Yang, Effects of driving behavior on real-world emissions of particulate matter, gaseous pollutants and particle-bound PAHs for diesel trucks, Environ. Pollut. 286 (2021) 117292.
[7] A.S.M. Bakibillah, M.A.S. Kamal, C.P. Tan, T. Hayakawa, J. Imura, Event-driven stochastic eco-driving strategy at signalized intersections from self-driving data, IEEE Trans. Veh. Technol. 68 (2019) 8557–8569.
[8] S. Wang, P. Yu, D. Shi, C. Yu, C. Yin, Research on eco-driving optimization of hybrid electric vehicle queue considering the driving style, J. Clean. Prod. 343 (2022) 130985.
[9] P. Fafoutellis, E.G. Mantouka, E.I. Vlahogianni, Eco-driving and its impacts on fuel efficiency: an overview of technologies and data-driven methods, Sustainability 13 (1) (2020) 226.
[10] P. Sun, D. Nam, R. Jayakrishnan, W. Jin, An eco-driving algorithm based on vehicle to infrastructure (V2I) communications for signalized intersections, Transp. Res., Part C, Emerg. Technol. 144 (2022) 103876.
[11] J. Ma, J. Hu, E. Leslie, F. Zhou, P. Huang, J. Bared, An eco-drive experiment on rolling terrains for fuel consumption optimization with connected automated vehicles, Transp. Res., Part C, Emerg. Technol. 100 (2019) 125–141.
[12] S. Su, J. She, K. Li, X. Wang, Y. Zhou, A nonlinear safety equilibrium spacing-based model predictive control for virtually coupled train set over gradient terrains, IEEE Transactions on Transportation Electrification 8 (2) (2021) 2810–2824.
[13] A.S.M. Bakibillah, M.A.S. Kamal, C.P. Tan, T. Hayakawa, J. Imura, Fuzzy-tuned model predictive control for dynamic eco-driving on hilly roads, Appl. Soft Comput. 99 (2021) 106875.
[14] K. Yeom, Model predictive control and deep reinforcement learning based energy efficient eco-driving for battery electric vehicles, Energy Rep. 8 (2022) 34–42.
[15] D. Llopis-Castelló, A.M. Pérez-Zuriaga, F.J. Camacho-Torregrosa, A. García, Impact of horizontal geometric design of two-lane rural roads on vehicle CO_2 emissions, Transp. Res., Part D, Transp. Environ. 59 (2018) 46–57.
[16] S. Zhu, B. Aksun-Guvenc, Trajectory planning of autonomous vehicles based on parameterized control optimization in dynamic on-road environments, J. Intell. Robot. Syst. 100 (2020) 1055–1067.
[17] C.J. Beckers, I.J. Besselink, H. Nijmeijer, Assessing the impact of cornering losses on the energy consumption of electric city buses, Transp. Res., Part D, Transp. Environ. 86 (2020) 102360.
[18] M. Ko, Incorporating vehicle emissions models into the geometric highway design process: application on horizontal curves, Transp. Res. Rec. 2503 (2015) 1–9.
[19] D.J. Chang, E.K. Morlok, Vehicle speed profiles to minimize work and fuel consumption, J. Transp. Eng. 131 (2005) 173–182.
[20] A. Fröberg, E. Hellström, L. Nielsen, Explicit fuel optimal speed profiles for heavy trucks on a set of topographic road profiles, SAE Technical Paper, Tech. Rep., 2006.
[21] P. Polterauer, G.P. Incremona, P. Colancri, L. del Re, A switching nonlinear MPC approach for ecodriving, in: Proc. American Control Conference (ACC), 2019, pp. 4608–4613.
[22] Y. Ikezawa, H. Fujimoto, D. Kawano, Y. Goto, Y. Takeda, K. Sato, Range extension autonomous driving for electric vehicle based on optimal vehicle velocity profile in consideration of cornering, Electr. Eng. Jpn. 207 (1) (2019) 899–907.
[23] J. Edrén, M. Jonasson, J. Jerrelind, A.S. Trigell, L. Drugge, Energy efficient cornering using over-actuation, Mechatronics 59 (2019) 69–81.
[24] F. Ding, H. Jin, On the optimal speed profile for eco-driving on curved roads, IEEE Trans. Intell. Transp. Syst. 19 (2018) 4000–4010.
[25] A. Bentaleb, A. El Hajjaji, A. Rabhi, A. Karama, A. Benzaouia, Energy-optimal control for eco-driving on curved roads, in: Proc. 2022 IEEE Intelligent Vehicles Symposium (IV), 2022, pp. 1584–1590.
[26] A. Kesting, M. Treiber, D. Helbing, Enhanced intelligent driver model to access the impact of driving strategies on traffic capacity, Philos. Trans. R. Soc. A, Math. Phys. Eng. Sci. 368 (1928) (2010) 4585–4605.
[27] J. Wang, H.A. Rakha, Fuel consumption model for heavy duty diesel trucks: model development and testing, Transp. Res., Part D, Transp. Environ. 55 (2017) 127–141.
[28] Y.T. Zhang, C.G. Claudel, M.B. Hu, Y.H. Yu, C.L. Shi, Develop of a fuel consumption model for hybrid vehicles, Energy Convers. Manag. 207 (2020) 112546.
[29] K. Ahn, H. Rakha, A. Trani, M. Van Aerde, Estimating vehicle fuel consumption and emissions based on instantaneous speed and acceleration levels, J. Transp. Eng. 128 (2) (2002) 182–190.
[30] H. Rakha, K. Ahn, A. Trani, Development of VT-micro model for estimating hot stabilized light duty vehicle and truck emissions, Transp. Res., Part D, Transp. Environ. 9 (2004) 49–74.
[31] Z. Yao, Y. Wang, B. Liu, B. Zhao, Y. Jiang, Fuel consumption and transportation emissions evaluation of mixed traffic flow with connected automated vehicles and human-driven vehicles on expressway, Energy 230 (2021) 120766.
[32] J. Du, H.A. Rakha, F. Filali, H. Eldardiry, COVID-19 pandemic impacts on traffic system delay, fuel consumption and emissions, Int. J. Transp. Sci. Technol. 10 (2) (2021) 184–196.
[33] P.J. Carlson, M. Burris, K. Black, E.R. Rose, Comparison of radius-estimating techniques for horizontal curves, Transp. Res. Rec. 1918 (2005) 76–83.
[34] S. Zamfir, R. Drosescu, R. Gaiginschi, Practical method for estimating road curvatures using onboard GPS and IMU equipment, Proc. IOP Conference Series: Materials Science and Engineering, IOP Publishing 147 (2016) 012114.
[35] I.H. Kim, J.H. Bong, J. Park, S. Park, Prediction of driver's intention of lane change by augmenting sensor information using machine learning techniques, Sensors 17 (6) (2017) 1350.